

Calculation of the insulator-set displacement induced by the ice and/or wind loads using 3D catenary equations

Borut Zemljarič

*Design Engineering Department, Elektro Gorenjska Company, Ulica Mirka Vadnova 3a, 4000 Kranj, Slovenia
E-pošta: borut.zemljarič@elektro-gorenjska.si*

Abstract. This paper presents a mathematical method to calculate the displacement of overhead-line conductors and suspension insulator sets during changeable conditions caused by ice and/or wind. The method which is consistent and mathematically transparent is primarily intended to be used in a 3D space to determine the initial conditions for a later more advanced dynamic calculation based on the finite element method. The method is based on the 3D catenary differential equations which for appropriate boundary conditions and insulator-set motion constraints form a mathematical system of algebraic-differential equations that are solved numerically. A numerical example shows that the method can be used with confidence as a simple alternative to other static methods or commercial softwares. Using the method, a wide spectrum of practical design problems associated with the overhead-line and ice and/or wind loads can be analyzed.

Keywords: insulators, displacements, transmission, overhead line, catenary, numerical method

Izračun pomikov izolatorjev s tridimenzionalnimi enačbami verižnice ob delovanju žlednih in vetrnih obtežb

Članek predstavlja matematično metodo za izračun pomikov izolatorskih sestavov in stanj verižnice visokonapetostnih daljnovodov, nastalih zaradi delovanja zunanjih vremenskih dejavnikov, predvsem žledne ali vetrne obtežbe na posamezne elemente daljnovoda. Predstavljena metoda je matematično transparentna in je namenjena predvsem za uporabo pri 3-D prostorskih problemih, ko moramo določiti začetne pogoje za reševanje zahtevnejših dinamične problemov. Ti po navadi temeljijo na metodi končnih elementov. Za ustrezno reševanje dinamičnih numeričnih integracij so natančni začetni pogoji nujni pogoj za doseganje konvergenč rešitev. Predstavljena matematična metoda temelji na tridimenzionalnih diferencialnih enačbah verižnice, ki skupaj z ustreznimi robnimi pogoji in enačbami mehanskih omejitev gibanja izolatorskih sestavov skupaj tvorijo sistem algebrajsko-diferencialnih enačb, ki ga moramo rešiti. Predstavljeni numerični rezultati kažejo, da je predstavljena metoda zanesljiva, in jo je mogoče uporabiti kot preprosto alternativo drugim metodam oziroma plačljivim komercialnim programskim paketom..

Ključne besede: izolatorji, pomiki, prenos, verižnica, numerične metode

Nomenclature

A- Conductor cross-section

a -Span length

b_0 -Perpendicular distance

C_E - Euler-transformation matrix

C_w -Wind-transformation matrix

C_1 - Vee-transformation matrix

C_{dt}, C_{dn}, C_{db} - Non-dimensional drag coefficients

d_0 - Conductor sag at $a/2$

D_c -Conductor diameter

D_a - Ice-load thickness on conductor

E – Young modulus of elasticity

F- Force vector

F_{ti}, F_{ni}, F_{bi} - Wind-force components

g- Gravitational constant

h -Vertical height distance

H- Horizontal conductor force

H_L, H_R - Horizontal force in the left- and right-hand side suspension point

J_k - I insulator-set weight

J_x, J_z - Vee insulator-set weight components

L_0 - Conductor stressed length

L_u - Conductor unstressed length

L_k, L_p, L_b - Hanging I, post and brace insulator lengths

m_k, m_p, m_b - Hanging I, post and brace insulator masses

m_c -Conductor mass per length

P_L, P_R - Perpendicular force in left- and right-hand side suspension point

r_x, r_z – Vee insulator gravity center components

s- Conductor unstressed material point

T_d - Drag force vector

T_L- Conductor tension vector

T_L - Conductor tension tangential component

t,n,b- Local conductor frame of reference vectors

U – Absolute wind velocity
 \mathbf{v}_r – Wind velocity vector
 v_{rt}, v_{rn}, v_{rb} – Wind components' relative velocity
 V – Vertical force
 V_L, V_R – Vertical force at left- or right-hand side suspension point
 w_L – Ice weight
 x, y, z – Coordinates in global frame of reference
 XYZ – Global frame of reference
 $X^1Y^1Z^1$ – Local frame of reference Vee insulator-set
 α – Angle between wind velocity and y, z plane
 $\mathbf{\Delta}$ – Displacements vector
 $\delta, \varepsilon, \eta$ – Components of displacements vector
 ρ – Air density
 θ, ϕ, ψ – Euler angles
 \mathbf{k} – Vector of geometric span data

1 INTRODUCTION

The development of new compact overhead power-transmission lines (OL) or reconstruction of the existing ones to decrease their visual impact on the landscape remains to be a very important aspect of the design process. One of the possible solutions involves the use of different types of insulator systems. Speaking in terms of the mechanical strength, it is important that when analyzing and designing such OLs, conductor sags, internal and external safety electrical distances and insulator shape, determined by using an appropriate design tool are considered in the calculation process.

While the OL static design is well known and supported by commercial software, to enable OL dynamic analysis, OL dynamic models must in most cases be developed and transformed to the software. Dynamic models based on the finite element methods (FEM) enabling a dynamic simulation, the initial conditions must be implemented. Usually, the commercial software is a closed black box from which the initial conditions needed for a dynamic model cannot be directly obtained. The paper presents a new numerical-mathematical approach to solving this issue. The method provides a tool to consider most of the used OL designs needing no special commercial software to establish the initial conditions to be used in dynamic simulations and analyses.

This paper deals with the problem of calculating the suspension-insulator sets displacement, caused by ice or wind loads or a combination of both. These loads can affect one or more spans of the high-voltage OL. An external load affecting a conductor changes its tensile force manifested as a displacement of a suspension-insulator set. When on insulator-set moves in a span with an increased conductor tensile force, the conductor force tends to reduce the span length and increases it in the adjacent spans. From its neutral position, the insulator set rotates to a new position, thus causing a conductor clip-in point displacement and giving rise to a

new conductor-insulator force equilibrium inside the OL tension field. No matter how simple is a vertically hanging insulator set, the calculation of a relatively simple problem is difficult as in addition to the ice load, the wind load too, must be taken into account. The impact of the wind load on the conductor turns a 2D problem into a three-dimensional (3D) problem where the catenary equation is not fully solved. The paper presents a consistent and mathematically transparent method to calculate the conductor displacements and sags induced by different ice or wind for an arbitrary shape of the insulator set.

Today, the usual approach to the problem solution and providing a corresponding software tool is using a method based on the conductor analytical catenary equation solved in 2D. The method is well presented by Kiesling et al. in [1]. They provide a physical understanding of the problem without considering the wind load in the mathematical model. Though not directly connected to our problem here, classical approaches to considering wind loads on a conductor are well presented by Peyrot et.al. [2]. Here in the development of a cable element, the solved catenary equation in 2D is still used. In the model, the conductor is virtually segmented into several elements and the wind pressure assumed to affect each element is constant and equal to that at the mid-length of the effected element. This concept is used in a common software tool [3]. The third concept comes from the field of dynamic problems where the commercial software, is based on the classical finite-element method (FEM). It used by Yan et al. [4] and McClure et al [5]. The conductor is divided into finite elements presented as beam elements by adding external ice and wind forces.

Unlike the existing methods which use an analytical conductor catenary solution in a 2D space or divide conductors into smaller elements, our method is directly based on differential cable equations in a 3D space. In searching for a numerical solution, we use the today's standard PCs and their numerical capabilities. We developed a relatively simple mathematical method using single-span differential equations developed by Blik [6]. For a multi-span conductor we developed a system of algebraic differential equations (ADEs) that mathematically describe the OL tension field. Another advantage of this method is that it can be used for any arbitrary insulator-set geometry.

The paper is organized as follows. Following this introduction, section 2 presents the span-displacement equilibrium equations used as the boundary conditions to solve the ADEs. Section 3 provides the conductor 3D governing static differential equations and includes the wind and ice loads as part of the conductor governing equations. Section 4 introduces the movement constraints expressed with displacement equations for a particular insulator set. Equations for the two most common insulator sets are presented. The first one is the classical vertical hanging I insulator and the second one

is the rotating Vee brace insulator set [7, 8]. Section 5 presents a numerical example and draws conclusions.

2 SPAN-DISPLACEMENT EQUILIBRIUM EQUATIONS

Let us consider that the OL consists of n spans. The conductor tension field is divided into n spans with suspension sets $i = 1, 2, \dots, n-1$, mounted on supporting towers. The first and the last tower are tension towers with a tension set. A single span with index i has a span length of a_{0i} , span height difference of h_{0i} , and span perpendicular distance of b_{0i} , as presented in Fig. 1. A global XYZ frame of reference is used. The subscript 0 indicates the OL initial state. This means that there are no external forces relating due to the ice or wind loads and the conductor horizontal force which is equal for all n -spans is H_0 . The initial span length and the vertical and perpendicular distances between the suspension points in the i -th span, written as a vector, are

$$\mathbf{\kappa}_{0i} = [a_{0i} \quad h_{0i} \quad b_{0i}]^T. \quad (1)$$

Consequently, at no ice or wind loads, all the insulator strings inside the tension field lie in the initial position. This state is taken as a reference position with the displacements equaling zero. Note that the conductors are clipped-in in the insulator sets. In Fig. 1, the initial states are shown with a continuous catenary line.

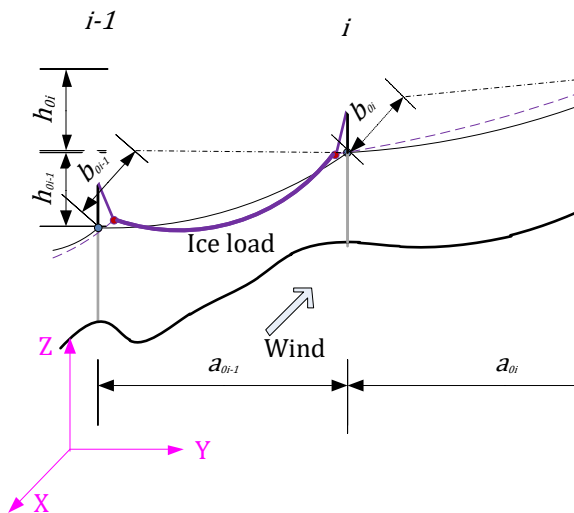


Figure 1. OL profile in the initial (continuous line) and displaced (dash line) state.

In most cases the initial position for the classical I insulator-set is in the vertical Z direction. The neutral position of the Vee brace insulator is in the X direction perpendicular to OL. The initial OL data and the initial conductor tension force allow us to calculate the conductor span length and sag using the classical catenary equation [1], [2], or, with an acceptable

accuracy, the parabola equation [9]. In the initial state, besides to the conductor horizontal tension force, only the gravitational force, determines the catenary shape inside individual spans. For OLs where the catenary profile is usually flat, the sag-to-span ratio is 1:8 or less, so for maximum conductor sag d_{0i} at the span mid-point and conductor length L_{0i} in single span i the following two equations apply

$$d_{0i} = m_c g a_{0i}^2 / 8H_{0i} \quad (2)$$

$$L_{0i} = \sqrt{h_{0i}^2 + \{a_{0i}[1 + (8/3)(d_{0i}/a_{0i})^2]\}^2}. \quad (3)$$

In (3), L_{0i} is the actual conductor stretch length for any initial temperature. As our focus is on the conductor-state changes caused by wind and/or ice forces, it is assumed that the temperature is constant. So, the conductor elongation and/or contraction due to temperature variations are omitted in the mathematical model. Besides the initial span data (1), by knowing unstressed conductor length L_{ui} as a supplement to horizontal tension force H_{0i} , the catenary equation is fully determined. Assuming that the tension in the conductor is constant throughout the span length, the unstressed conductor length gives the following equation adopted from [2]

$$L_{ui} = L_{0i} \left(1 - \frac{H_{0i} L_{0i}}{AE h_{0i}} \right). \quad (4)$$

At this point, we define force vector \mathbf{F} acting on the insulator-set suspension point with the components defined in the global frame of reference. Inside the i -th span on the left-hand side end suspension point and equally on the right-hand side and suspension point, the forces are

$$\mathbf{F}_{Li} = [H_{Li} \quad V_{Li} \quad P_{Li}]^T, \quad \mathbf{F}_{Ri} = [H_{Ri} \quad V_{Ri} \quad P_{Ri}]^T. \quad (5)$$

For a moment, we must assume that force vectors (5) are known. However, when the conductor condition is changed by a wind or ice load, the conductor tensile forces change in all the spans. If the conductor suspension points in a span move, the higher tensile force moves the suspension points in these directions and consequently changes the span data in the adjacent spans as shown in Fig. 2 and illustrated with a dotted catenary line in Fig. 1.

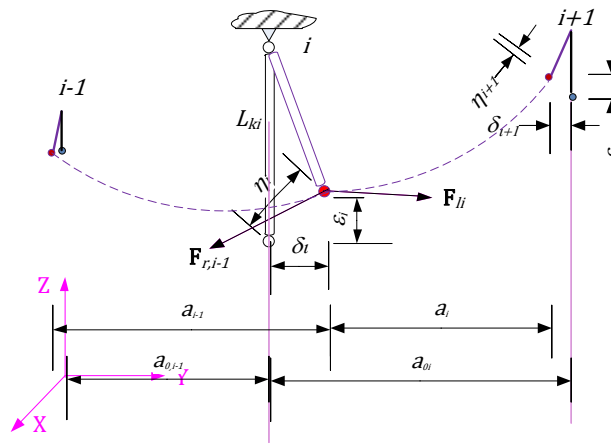


Figure 2. Displacements of the I insulator from its initial position.

The newly shaped catenary data with the displaced insulator-set for an i -th span can be written in the following vector form

$$\mathbf{\kappa}_i = [a_i \quad h_i \quad b_i]^T. \quad (6)$$

Displacements vector Δ_i of an i -th insulator suspension set with horizontal δ_i , vertical ε_i , and perpendicular η_i components in the global frame of reference for a single suspension set is

$$\Delta_i = [\delta_i \quad \varepsilon_i \quad \eta_i]^T. \quad (7)$$

The displacement is caused by the difference in the forces effecting the conductor from adjacent spans i and $i - 1$ in the supporting point as the new equilibrium of moments is set. The force-difference vector at the suspension point is

$$\mathbf{F}_i = [H_i \quad V_i \quad P_i]^T = \mathbf{F}_{Ri-1} - \mathbf{F}_{Li}. \quad (8)$$

The displacement vector (7) in fact describes a an enforced insulator-set movement and is given by the kinematics of the chosen suspension-set type. The displacement equations can be derived for any suspension-set geometry, as we will show later in Section 4. Besides the given material and the geometrical insulator-set data (weight, insulator dimensions, constraints) that are constants, the displacement is only a function of the resultant forces (8) in the suspension point. So $\Delta_i = \Delta_i(\mathbf{F}_{Li}, \mathbf{F}_{Ri})$. Note that the conductor force at the conductor end (5) and the catenary data (6) are also determined and can be viewed as a function of $\mathbf{\kappa}_i = \mathbf{\kappa}_i(\mathbf{F}_{Li})$. Referring to Fig. 2, the following vector equation holds for all spans

$$\mathbf{\kappa}_{0i} + (\Delta_{i+1} - \Delta_i) - \mathbf{\kappa}_i = \mathbf{0} \quad i = 1, 2, \dots, n. \quad (9)$$

Equation (9) which describes the boundary conditions to be met when searching for the algorithm, is only a function of the conductor tension forces. By

determining the conductor forces in an individual span that satisfies equation (9), the displacement in a static configuration can be calculated by taking into account the wind and/or ice loads for an arbitrary span.

3 3D CONDUCTOR STATIC EQUATIONS

In this section, equations are given to calculate the new span data (6) and the adjacent span resultant forces (8) in the suspension point. At this point our approach differs significantly from the existing methods. The forces are calculated directly with differential 3D catenary equations developed in [6]. They are extracted a static solution of the original dynamical equation describing 3D conductor motions in a single span. Using them under a static condition, the single-span catenary is fully determined with seven ADEs written in the conductor natural frame of reference fixed on the conductor and expressed in terms of the Euler angles. After minor adaptations to better fit our problem and adding the ice load and ice thickness variables, the equations are summarized as the governing equations

$$\begin{aligned} \frac{\partial T_i}{\partial s_i} + F_{Ti} - (m_c g + w_{Li}) \sin \phi_i &= 0 \\ \frac{T_i}{\cos \psi_i} \frac{\partial \phi_i}{\partial s_i} + F_{ni} - (m_c g + w_{Li}) \cos \psi_i \cos \phi_i &= 0 \\ F_{bi} + (m_c g + w_{Li}) \sin \psi_i \cos \phi_i &= 0 \\ \frac{T_i \cos \phi_i}{\sin \psi_i} \frac{\partial \theta_i}{\partial s_i} - F_{ni} + (m_c g + w_{Li}) \cos \psi_i \cos \phi_i &= 0 \end{aligned} \quad (10a)$$

and as the geometrical equations

$$\begin{aligned} \frac{\partial y_i}{\partial s_i} &= \left(1 + \frac{T_i}{EA}\right) \cos \theta_i \cos \phi_i = 0 \\ \frac{\partial z_i}{\partial s_i} &= \left(1 + \frac{T_i}{EA}\right) \cos \theta_i \sin \phi_i = 0 \\ \frac{\partial x_i}{\partial s_i} &= -\left(1 + \frac{T_i}{EA}\right) \sin \theta_i \cos \phi_i = 0. \end{aligned} \quad (10b)$$

Parameter s_i is an un-stressed material point on the conductor. Not going into detail, Euler angles ϕ_i , θ_i , ψ_i define the position of the local $\mathbf{t}, \mathbf{n}, \mathbf{b}$ frame of the reference relative to global frame of reference XYZ, (see Fig. 3).

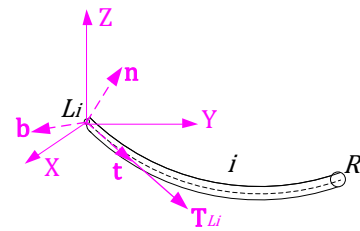


Figure 3. Conductor global and local frame of reference.

In the natural frame of reference, the conductor ends have only the tangential component in the direction of vector \mathbf{t} , which is on the conductor either left- or right-hand side, equal to T_{Li} , or T_{Ri} . In a vector form, both sides are defined as $\mathbf{T}_{Li} = [T_{Li} \quad 0 \quad 0]^T$ and $\mathbf{T}_{Ri} =$

$[T_{Ri} \ 0 \ 0]^T$. Using the transformation matrix \mathbf{C}_E given in the Appendix, the transformations between the local and global force (5) components are

$$\mathbf{F}_{Ri} = \mathbf{C}_E^{-1} \mathbf{T}_{Ri} \text{ or } \mathbf{F}_{Li} = \mathbf{C}_E^{-1} \mathbf{T}_{Li}. \quad (11)$$

In the governing equations (10a), the external drag-force components per unit length F_{ti} , F_{bi} , F_{ni} induced by the wind force on the conductor are directly included in the equations. In a vector form, the drag force on the conductor in the local frame of reference is defined as

$$\mathbf{T}_{di} = [F_{ti} \ F_{bi} \ F_{ni}]^T. \quad (12)$$

At this point it is also necessary to consider two aspects of the OL wind load discussed in the literature. The first aspect provides an insight into the related design standards [10] imposed on the inclusion of the wind velocity as an external OL load in the design process. The wind force is calculated using simplified equations and applicable tables showing the wind coefficients. The second aspect deals with the mechanic-dynamic phenomena such as Aeolian vibrations, sub-span oscillations and galloping conductors [11-15]. The wind force acting on a conductor is calculated as a classical drag-force response to the wind velocity. So, equations [6] can also be used in our numerical model, similarly as in the above-mentioned references. In a quasi-static state, the relative wind velocity is the same as the wind velocity. Assuming that the wind blows horizontally in the XY plane with velocity U and defining angle α between the wind direction and the YZ plane, the components of the wind-induced forces are:

$$\begin{aligned} F_{ti} &= -\frac{1}{2} \rho C_{dt} (D_c + 2D_{ai}) v_{rti} |v_{rti}| \left(1 + \frac{2T_i}{EA}\right) \\ F_{ni} &= -\frac{1}{2} \rho C_{dn} (D_c + 2D_{ai}) (v_{rni}^2 + v_{rbi}^2)^{\frac{1}{2}} v_{rni} \left(1 + \frac{2T_i}{EA}\right) \\ F_{bi} &= -\frac{1}{2} \rho C_{db} (D_c + 2D_{ai}) (v_{rni}^2 + v_{rbi}^2)^{\frac{1}{2}} v_{rbi} \left(1 + \frac{2T_i}{EA}\right) \end{aligned} \quad (13)$$

In Eq. (13), the vector of relative wind velocity \mathbf{v}_{ri} is defined in the local frame of reference with the components $\mathbf{v}_{ri} = [v_{rti} \ v_{rni} \ v_{rbi}]^T$. Knowing wind velocity U and wind-blowing angle α in the global frame using wind-transformation matrix \mathbf{C}_w given in the Appendix, the relative components in the local frame of reference expressed in terms of the Euler angles are

$$\mathbf{v}_{ri} = \mathbf{C}_{wi} U. \quad (14)$$

A brief comment on ice weight w_{Li} and ice thickness D_{ai} included in (10a) and (10b) should be made. In general, they are both chosen arbitrarily.

For individual span i , a system of seven equations (10a and 10b) with seven unknowns needs to be solved. In n -span tension field, an equation system consisting of $n * 7$ sets of ADEs is created. Each single-span

integration interval is determined by the conductor unstressed length (4) in interval $[0 \ L_{ui}]$. The results of integrating the governing relations (10a) in individual spans are the conductor tension force and Euler angles. By simultaneously integrating the geometrical relations (10b), individual span data $\mathbf{\kappa}_i$ are calculated. They depend on the conductor tension force and Euler angles. As an example, integrating the first geometrical equation gives the horizontal span length of $a_i = \int_0^{L_{ui}} \left(1 + \frac{T_i}{EA}\right) \cos \theta_i \cos \phi_i \, ds_i$. The same is true for the second and third geometrical equation and the results are h_i and b_i . Note that, by using algebraic equation third angle ψ_i can be expressed with the other two Euler angles. To solve the system equation (9), an iterative method is needed. It can be a shooting method or any software pre-built numerical method able to solve an ADE system. We shoot to T_i , ϕ_i , θ_i , and integrate the geometrical equation to obtain the span and displacement data for the current iterations. The iterations continue until (9) is satisfied. Note that the data (a_i, h_i, b_i) of span is an integral boundary condition and corresponds to three unknowns per span, i.e one is the force and two are the Euler angles. Finally, to solve (9), the insulator displacement equation Δ_i as a function of the force vector is determined as shown in the next section.

4 INSULATOR SET-DISPLACEMENT

Two of the most used insulator types will be discussed. However, it should be mentioned that the presented method is open for any insulator-set geometry. For presentation purposes, we chose the hanging I insulator-set and the Vee insulator-set. It should be made clear that the displacement equations are developed for a particular insulator type. By changing equation set (8), it is easy to move between the different insulator types in the mathematical model. The insulator-set rotation is a kinematically constrained movement. In the paper we present the final results derived from the moments and the constrained equations.

4.1 I insulator set

Referring to Fig. 2, the displacement vector components in the global frame of reference for the vertical I insulator string of length L_k and insulator weight J_k give the equations

$$\begin{aligned} \delta_i &= L_k \frac{H_i}{\sqrt{H_i^2 + \left(\frac{J_k}{2} + V_i\right)^2 + P_i^2}} \\ \varepsilon_i &= L_k \left(1 - \frac{-\left(\frac{J_k}{2} + V_i\right)}{\sqrt{H_i^2 + \left(\frac{J_k}{2} + V_i\right)^2 + P_i^2}}\right) \\ \eta_i &= L_k \frac{P_i}{\sqrt{H_i^2 + \left(\frac{J_k}{2} + V_i\right)^2 + P_i^2}}. \end{aligned} \quad (15)$$

Taking the wind force as zero, the equation reduces to a 2D case with the same equations as in [1].

4.2 Vee insulator set

As the Vee insulator set is more complex, the basic steps towards displacement equations are outlined to show the calculation principle. A typical Vee-braced insulator-set is given in Fig. 4a.

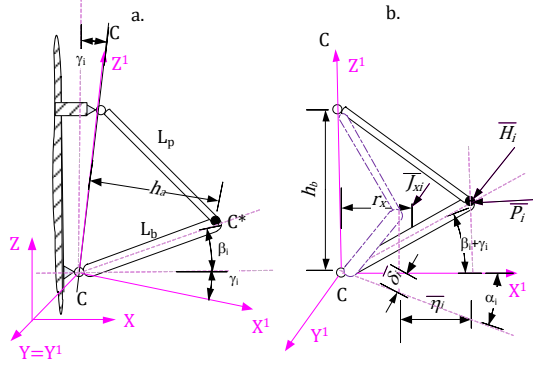


Figure 4. Vee insulator set (a. initial position, b. mathematical model in a local frame of reference).

The insulator-set assembly consists of two basic elements. A post insulator of length L_{pi} and mass m_{pi} mounted at inclination β_i to the horizontal X global axis. The brace insulator has length L_{bi} and mass m_{bi} . The post and brace part hang at points on the rotation CC axis. The CC axis has inclination γ_i to the vertical Z axis. The assembly has a rigid connection between the elements at point C^* and freely rotates around the CC axis. The first calculating step in calculating the displacement is introducing the local frame of reference, $X^1 Y^1 Z^1$, rotated by γ_i around the Y axis, as presented in Fig. 4b. The values in the $X^1 Y^1 Z^1$ frame of reference are written with a dashed upper script. The relation between the global and the local frame of reference now defines transformation matrix \mathbf{C}_1 given in the Appendix. Using the local frame of reference, the problem is simplified to triangular kinematics, where self-insulator set weight \bar{J}_{xi} acts on the triangular gravity center and together with resultant force $\bar{\mathbf{F}}_i$ at point C^* rotates the assembly. The calculation for the gravity center and self-weight is given in the Appendix. The conductor forces expressed in local frame of references expressed with the global forces are

$$\bar{\mathbf{F}}_i = [\bar{H}_i \quad \bar{V}_i \quad \bar{P}_i]^T = \mathbf{C}_1 \mathbf{F}_i. \quad (16)$$

It is obvious that in the local frame of reference there are only two displacement components exists, the third one is identical to zero. Writing only the results of the equation derivation, vector $\bar{\Delta}_i = [\bar{\delta}_i \quad \bar{\varepsilon}_i \quad \bar{\eta}_i]^T$ with components is

$$\begin{aligned} \bar{\delta}_i &= h_{ai}^2 \frac{\bar{H}_i}{\sqrt{(h_{ai}\bar{H}_i)^2 + (\bar{r}_{xi}\bar{J}_{xi} + h_{ai}\bar{P}_i)^2}} \\ \bar{\varepsilon}_i &= 0 \\ \bar{\eta}_i &= h_{ai} \left(1 - \frac{-(\bar{r}_{xi}\bar{J}_{xi} + h_{ai}\bar{P}_i)}{\sqrt{(h_{ai}\bar{H}_i)^2 + (\bar{r}_{xi}\bar{J}_{xi} + h_{ai}\bar{P}_i)^2}} \right). \end{aligned} \quad (17)$$

Finally, back from the local to the global frame of reference with the transformation in the vector form they are

$$\Delta_i = \mathbf{C}_1^{-1} \bar{\Delta}_i \quad (18)$$

A similar approach is used to prepare the displacement equations for another insulator-set assembly.

5 NUMERICAL EXAMPLE

To verify and demonstrate the usefulness of our mathematical method, the method is used for a practical designer problem, where the differences between the OL equipped with a classical I insulator-set or with Vee insulator-set are analyzed. In the numerical example, the results attained with our method and those calculated with the commercial software [3] are compared. The calculations are performed on PC in a self-developed software program based on the MatLab platform. As the presented method uses the numerical calculations, the initial conditions for solving ADE are necessary. The testing problems can be solved within in the range of a normal ice load and/or wind load up to 15 m/s using the following rough initial assumptions

$$\begin{aligned} T_i &\sim (L_i - L_{0i}/L_{0i})EA \\ \phi_{0i} &\sim \tan^{-1}(2(h_i - d_i)/a_i) \\ \theta_{0i} &= \tan^{-1}(Ud_i/m_i g). \end{aligned} \quad (19)$$

At higher wind speeds, a higher initial accuracy or step calculation is needed to achieve iteration convergence to a solution. To overcome the convergence problem, the loads should be divided into smaller parts and more calculation steps should be taken for the solution. In the numerical example, the ACSR 240/40 conductor is strung in a tension field consisting of four spans with the lengths of 257m, 270m, 260m and 245m and three insulator-sets I1, I2, I3. The height differences between the span suspension points are 0m, 0m, -4m, and -2m, and OL is a straight line. The horizontal conductor tension is 22.6 kN. The conductor mass per unit length is 0.98 kg/m, the cross-section is 282.5 mm², the diameter is 21.8 mm and the Young's modulus is 77,000 N/mm². The mass of the classic I insulator-set is 15 kg and the length is 2m. In the Vee insulator set, the length of the post insulator is 1.4 m, the mass is 15 kg and inclination to the horizontal axis is 12°. The length of the brace insulator part is 1.6 m, the mass is 5 kg.

Table I summarizes the comparison results for the two calculation methods and two insulator-set types. The three cases, A, B and C, are included in the table. In case A an ice load of the weight of 15 N/m is only in the second span where there is no wind pressure. In case B ice load condition is the same and the speed of a perpendicular wind is 10 m/s at all spans and at the air density of 1.225 kg/m³. Case C is the same as case B with the exception of the wind which here attacks at a 30° angle to the OL. Table I shows a good agreement

between the compared calculation methods for the two insulator types in each sub-case. The small differences of 10% in the longitudinal direction is likely to be due to the different numerical models. The accuracy

obtained on the basis of tailored initial conditions, enables a direct and converging numerical calculation.

Table 1: Results of a comparison between the two calculation methods

	INSULATOR-SETS						VEE INSULATOR-SETS					
	PRESENTED METHOD DISPLACEMENTS			SAPS SOFTWARE DISPLACEMENTS			PRESENTED METHOD DISPLACEMENTS			SAPS SOFTWARE DISPLACEMENTS		
	Y	Z	X	Y	Z	X	Y	Z	X	Y	Z	X
	(m)	(m)	(m)	(m)	(m)	(m)	(m)	(m)	(m)	(m)	(m)	(m)
<i>A. Ice load in second span.</i>												
I1	0.131	0.004	0	0.123	0.003	0	0.132	0.001	-0.007	0.124	0.000	-0.006
I2	-0.206	0.011	0	-0.227	0.012	0	-0.214	0.004	-0.018	-0.236	0.004	-0.022
I3	-0.107	0.003	0	-0.107	0.003	0	-0.111	0.001	-0.009	-0.112	-0.000	-0.005
<i>B. Ice load and perpendicular wind.</i>												
I1	0.131	0.015	-0.211	0.123	0.014	-0.212	0.132	0.001	-0.006	0.124	0.000	-0.006
I2	-0.205	0.021	-0.204	-0.227	0.023	-0.205	-0.212	0.004	-0.017	-0.239	0.004	-0.022
I3	-0.106	0.019	-0.259	-0.107	0.019	-0.260	-0.110	0.001	-0.005	-0.113	-0.000	-0.004
<i>C. Ice load and wind under 30°.</i>												
I1	0.138	0.005	-0.053	0.123	0.004	-0.053	0.139	0.002	-0.007	0.124	0.000	-0.006
I2	-0.194	0.010	-0.052	-0.227	0.013	-0.051	-0.199	0.003	-0.015	-0.236	0.004	-0.022
I3	-0.099	0.004	-0.066	-0.107	0.004	-0.066	-0.102	0.001	-0.004	-0.112	-0.000	-0.005

The main goal of this paper is to compare the methods. Analyzing the differences between the two insulator types is left to the reader.

6 CONCLUSION

The numerical example shows that the presented method can be used with confidence by OL designers as a simple alternative to other known methods or commercial software to calculate a new conductor state induced by ice and/or wind loads. Primarily, the method is developed to calculate the initial conditions needed for the dynamic FEM based calculations. It is general and mathematically transparent and can be viewed as an alternative when tailored input data for solving special problems must be determined and no commercial software is available.

Though the aim of this paper is to investigate the insulator-set displacement, the output of the presented method are sags, forces and other data important for the designer work. The method can be upgraded for any insulator-set shape by developing the designers own displacement equations and simply adding them to the library. Besides calculating initial conditions for the FEM methods, the method can be applied to a wide spectrum of practical problems to analyze different OL issues and to provide either compact or classical solutions.

7 APPENDIX

7.1 Euler-transformation matrix

Transformation from the conductor global (XYZ) frame of reference to the local (natural $\mathbf{t n b}$) frame of reference using the Euler angles with rotating sequence $Y, Z, X/\theta, \phi, \psi$

$$\mathbf{C}_E = \begin{bmatrix} \cos \theta_i \cos \phi_i & \sin \phi_i \\ \sin \psi_i \sin \theta_i - \cos \psi_i \sin \phi_i \cos \theta_i & \cos \psi_i \cos \phi_i \\ \cos \psi_i \sin \theta_i + \sin \psi_i \sin \phi_i \cos \theta_i & -\sin \psi_i \cos \phi_i \\ -\sin \theta_i \cos \phi_i & \\ \sin \psi_i \cos \theta_i + \cos \psi_i \sin \phi_i \sin \theta_i & \\ \cos \psi_i \cos \theta_i - \sin \psi_i \sin \phi_i \sin \theta_i & \end{bmatrix}. \quad (20)$$

7.2 Wind-transformation matrix

The wind transformation matrix is

$$\mathbf{C}_w = \begin{bmatrix} \cos(\theta_i - \alpha) \cos \phi_i \\ -\sin(\theta_i - \alpha) \sin \psi_i - \cos(\theta_i - \alpha) \sin \phi_i \cos \psi_i \\ \sin(\theta_i - \alpha) \cos \psi_i + \cos(\theta_i - \alpha) \sin \phi_i \sin \psi_i \end{bmatrix} \quad (21)$$

7.3 Vee-transformation matrix

The transformation matrix from the global (XYZ) to the insulator local ($X^1Y^1Z^1$) frame of reference is

$$\mathbf{C}_1 = \begin{bmatrix} 1 & 0 & 0 \\ 0 & \cos \gamma_i & -\sin \gamma_i \\ 0 & \sin \gamma_i & \cos \gamma_i \end{bmatrix} \quad (22)$$

7.4 Gravity center of the Vee insulator-set

The insulator weight vector and gravity center vector in the local frame of reference are

$$\bar{\mathbf{J}}_i = [\bar{J}_{zi} \quad 0 \quad \bar{J}_{xi}]^T = \mathbf{C}_1 [-g(m_{pi} + m_{bi}) \quad 0 \quad 0]^T$$

$$\bar{\mathbf{r}}_{ci} = [0 \quad \bar{r}_z \quad \bar{r}_x]^T = \frac{1}{m_{pi} + m_{bi}} [m_{pi} \bar{\mathbf{r}}_{cpi} + m_{bi} \bar{\mathbf{r}}_{cbi}] \quad (23)$$

where the geometrical values are

$$h_{ai} = L_{pi} \cos(\beta_i + \gamma_i)$$

$$h_{bi} = L_{pi} \sin(\beta_i + \gamma_i) + \sqrt{L_{bi}^2 - h_{ai}^2}$$

and the local gravity centers for the post and brace parts separately are

$$\bar{\mathbf{r}}_{cpi} = \left[0 \quad \frac{L_{pi}}{2} \sin(\beta_i + \gamma_i) \quad \frac{h_{ai}}{2} \right]^T$$

$$\bar{\mathbf{r}}_{cbi} = \left[0 \quad \frac{1}{2}(h_b + L_{pi} \sin(\beta_i + \gamma_i)) \quad \frac{h_{ai}}{2} \right]^T.$$

REFERENCES

- [1] F. Kiessling, P.Nefzger, J.F.Nolasco, U. Kaintzyk, "Overhead Power Lines", Springer, 2003, p. 539-571.
- [2] A.H. Peyrot, A.M. Gaulois, "Analysis of flexible transmission lines", Journal of structural division, 1978, Vol. 104, No. St5, p. 763-779.
- [3] Software manual, "SAPS-Version 7", Power line systems, Inc, 2006.
- [4] B.Yan, X.Lin, W. Luo, Z.Chen, Z.Liu, "Numerical study on Dynamic Swing of Suspension Insulator string in overhead transmission line under wind load", IEEE Transaction on power delivery, 2010, Vol.25, No. 1, p. 248-259.
- [5] G.McClure, M.Lapointe, "Modeling the structural dynamic response of overhead transmission lines", Computers and Structures, 2003, Vol.81, p. 825-834.
- [6] A. Blied, "Dynamic analysis of single span cables", PhD, Massachusetts institute of technology, 1984.
- [7] A.C.Baker, P.E.Murray, J.D.Mozer, "Computer aided analysis of wind loads on horizontal Vee type transmission line systems", IEEE Transactions on Power apparatus and systems, 1982, Vol.PAS-101, No. 8, p. 2415-2419.
- [8] D.Dumora, D. Feldmann, M.Gaudry, "Mechanical behavior of flexurally stressed composite insulators", IEEE Transaction on power delivery, 1990, Vol.5, No.2, 1990, p. 1066-1073.
- [9] H.M.Irvine, "Cable structures", MIT press, 1981.
- [10] Standard EN 50341-1: 2012, "Overhead electrical lines exceeding AC 1kV-Part 1: general requirements", Cenelec
- [11] H.Keyhan, G. McClure, W. Habashi, "On computational modeling of interactive wind and icing effects on overhead line conductors", The 14th Workshop on atmospheric icing of structures, 2011, Chongqing
- [12] O. Nigol, P.Buchan, "Conductor galloping Part-1- Den Hartog mechanism", IEEE Transaction on Power apparatus and systems, 1981, Vol. PAS.100, No.2, p. 699-707
- [13] J. Wang, J. Lilien, "Overhead electrical transmission line galloping", IEEE Transaction on power delivery, 1998, Vol.13, No. 3, p. 909-916

[14] N. Impollonia, G. Ricciardi, F. Saitta, "Vibrations of inclined cables under skew wind, International journal of Non-Linear Mechanics, 2011, doi:10.1016/j.ijnonlinmec.2011.03.006

[15] F. Williams (2006), "Dynamics of a cable with an attach sliding mass", ANZIAM J.47 (EMAC2995), C86-C100

Borut Zemljarič je diplomiral leta 1994 in magistriral leta 2008 na Fakulteti za elektrotehniko v Ljubljani. Deluje v okviru gospodarske družbe, na mestu projektanta visokonapetostnih povezav in naprav. Njegova raziskovalna zanimanja poleg elektromagnetnih polj obsegajo tudi razvoj numeričnih metod, namenjenih proučevanju dinamičnih mehanskih stanj daljnovidov v ekstremnih vremenskih razmerah.